https://doi.org/10.2352/ISSN.2470-1173.2021.3.MOBMU-143

The potential of NIR spectroscopy in the separation of plastics for pyrolysis

Uduak Bassey [1], Lukasz Rojek [1,3], Michael Hartmann [1], Reiner Creutzburg [1,2] and Arne Volland [4].

[1] SRH Berlin University of Applied Sciences, Berlin School of Technology, Ernst-Reuter-Platz 10, D-10587 Berlin, Germany

[2] Technische Hochschule Brandenburg, Department of Informatics and Media, IT- and Media Forensics Lab, Magdeburger Str. 50, D-14770 Brandenburg, Germany

[3] Beuth University of Applied Sciences, Berlin, Luxemburger Straße 10, D-13353 Berlin, Germany

[4] LLA Instruments GmbH & Co. KG, Justus-von-Liebig-Straße 9/11, D-12489 Berlin, Germany

E-mails: uduak.bassey@srh.de; lukasz.rojek@srh.de; michael.hartmann@srh.de; reiner.creutzburg@srh.de; a.volland@lla.de

Abstract

The present-day substantial growth in the demand and utilization of plastics provokes severe economic and environmental consequences. Around 4 – 6 % of global oil and gas production is used directly or indirectly as feedstock in the production of plastics. A further 2 – 3 % is employed as energy during the manufacturing process.

This study highlights recycling (chemical) against other sustainable waste management approaches, like mitigation of waste generation through the concept of reusing and energy recovery from plastics. As an example, the African context regarding the quality of the disposed waste and the waste characteristics in the Kumasi region, Ghana is taken into consideration.

To process valuable and economically viable recycling products, pure polymers are required. Certain technologies, such as infrared (IR) spectroscopy, have limitations for accurately identifying different polymer types, particularly when the sample mix is contaminated with organic waste or is physically wet. There are promising technologies that are under development, like Raman spectroscopy and laser-aided spectroscopy combined with tracers (fluorescent markers). Nonetheless, these are essentially more expensive technologies and are currently in the development phase.

Multiplexed near-infrared (NIR) spectroscopy is a fitting technology for polymer identification. It is a fast and non-destructive technique that does not influence the physical state nor chemical property of the sample polymers. Hence, it can be integrated in a continuous sorting system. Here, a prototype sorting system equipped with a multiplexed NIR spectrometer was utilized and used to test the sorting efficiency of the system as well as the purity of identified and sorted samples. Samples of PE (with subgroups of HDPE, LDPE and LLDPE), PS, PET, PP and PVC and unknown polymers were employed in several conditions. The measurements were carried out in real time, based on the speed of the conveyor belt. In this study, a novel setup is introduced and investigated, and its data analyzed to determine the reliability of the sorting method for plastics to be used for pyrolysis.

Introduction

Plastics have become one of the most popular materials and it directly influences our daily lives. It is relevant in several sectors like packaging, transportation, construction, electronic manufacturing, and in recent years, energy. This has induced a steady growth in plastics with annual global production reaching 407 million tons [1]. With the current growth trend in plastics production, it is projected that by 2050, global annual production will reach 1.6 billion metric tons per annum [2]. As plastics production increases, there is a corresponding increase in plastics waste generated.

In Africa for instance, the estimated plastics waste generation for the continent in 2015 was 19.5 million tons [3]. From this estimated figure, only 12% is recycled while more than 80% is inadequately disposed of and pose an active risk of polluting water bodies [4]. This is evident in the global distribution of plastics waste that is mismanaged and input to the oceans. Recent studies shows that 1/8 of waste plastics entering the ocean per year is from African countries [5]. Research has indicated that it takes 100 years for plastics to degrade. Within this time frame, plastics break-down into potential hazardous macro plastics (> 5 mm), micro plastics (< 5 mm) and nano plastics (< .001 mm) [6], which can be consumed by marine organisms. Subsequently, the aquatic eco-system could be threatened and could consequently have a direct impact on human health [7].

Contrastingly, the potential of post-consumer plastics is enormous, taking into context the energetic and economic value. According to Business Informatics Research (BIR), a ton of recycled plastics is equivalent to 2604 liters of crude-oil and can mitigate energy consumption of plastics production by 80% – 90%, compared to plastics production from its raw-material [1]. A ton of recycled plastics is equivalent to 22 cubic meters of waste plastics that could potentially end up in a landfill [1]. Plastics recycling offers huge potentials. The current global recycling rate lies between 14% and 19%, 24% of plastics waste is either incinerated or disposed of in landfills, while 58% - 62% are disposed of in the natural environment. However, in 2018, the United Nations estimated the global recycling rate for plastics at just 9% [1]. Plastics recycling rate in Ghana, West-Africa has hovered between 1% and 6% in recent years [8]. This has remained low due to two

factors: the heterogenous nature of waste disposal (all waste fractions dumped together), and the high fraction of organic wastes. With the fraction of organic waste ranging from 48% - 69% depending on the region [9], plastics separation that enables recycling already faces huge challenges. Consequently, in 2015, the country was ranked the 7th dirtiest in the world [10]. Additionally, a huge fraction of the waste plastics is deposited in landfills. However, there is scarcely any energy recovery from waste plastics, largely due to inefficient separation arising from the condition of waste plastics recovered from landfills.

Plastics wastes globally consists of a wide variety of polymers. However, the largest quantities are represented by polyethylene subgroups (HDPE, LDPE and LLDPE, 30%), polypropylene (PP, 19%), polyethylene terephthalate (PET, 7%) and about 10% of polyvinyl chloride (PVC) [11]. Potential high value products can be obtained from the wide variety of polymers found in plastics wastes, if properly managed. Polyolefins[1], for instance, can produce high value products after pyrolysis. Some of the potential products obtained from plastics polymers after pyrolysis are listed in table 1 below.

Table 1: Obtained products from different plastics resins (source: ([12],[13])

Resin	Low-temperature products	High-temperature products
PE	waxes, paraffin, oils, α-olefins	gases, light oils
PP	Vaseline, olefins	gases, light oils
PVC	HCl, benzene	toluene
PS	styrene	styrene
PET	benzoic acid, vinyl terephthalate	TFE

Based on these facts, there is an urgent need to improve the current waste management strategy, particularly in waste plastics management focused on separation and recovery.

The vast potential of waste plastics invokes the question of the best method required to exploit these potentials. Separation is instrumental to the process of harnessing the potential of post-consumer plastics. It involves the segregation of plastics into the different polymer types. The major success of recycling or recovering materials (with regards to environmental and economic efficiency) at the end of their life cycle depends greatly on the reliability of the separation process utilized. The sorting process must be effective in differentiating between types, grades and possibly quality of plastics in a cost-effective and rapid manner such that the incurred cost is less than the value of the recycled product [14]. To improve the rate and reliability of the plastics sorting process based on economic performance, automated sorting processes are utilized, in which end-of-life polymer products are sorted based on size (macro/micro-sorting) [15], density, molecular structure and other identification characteristics. Automated sorting systems which is ideal and poses the least risk (health) mostly rely on intrinsic and extrinsic property of the polymers such as physical, chemical, optical, molecular structure or the electrostatic capability of the materials [16].

The most common automatic sorting method is density separator which relies on the density of a medium and sorts out samples into two categories namely, float products and sink products. The float products have density less than the medium while the sink products have a higher density than the medium. This method is not useful to separate plastics based on their polymer type. Optical sorting offers a more promising method of separating plastics based on their polymer types. It involves the use of sensors to detect the color, shape, size molecular and chemical structure of an object. The sensors can detect these attributes using software-propelled intelligence [17]. The software operates by comparing the sample's (polymer's) attribute to user-defined accept or reject criteria. If the attribute matches with the accept criteria, the polymer is identified. Intelligent software's will group several matching attributes into learning sets to improve identification. The optical sorter requires the combination of lights and sensors. The lights, illuminates and radiates photon on the sample at a certain frequency, while the sensors detect the reaction of the polymer to the light. The sensors can capture the refection, absorption, and even molecular vibrations of the polymers to the light (energy source). There are several optical technologies that are used in the classification of polymers, some examples are: Raman spectroscopy [18], laser spectroscopy [19], x-ray fluorescence [20], infrared spectroscopy [21]. These methods, such as laser spectroscopy and x-ray fluorescence are only applicable with newly manufactured plastics, as they rely on trace elements present in the polymer for successful identification. Infrared spectroscopy has a slow response during measurement due to the weak radiation in this spectral range, different materials could fully absorb this weak radiation which would consequently present unreliable results. Raman spectroscopy offers a huge potential in waste plastics identification and separation; however, it is still in its pilot phase of development and still requires a lot of research to improve calibration results and building of chemometric library. Additionally, the Raman effect is weak, therefore, it requires a highly sensitive and expensive detection mechanism [22]. With the growing concern of plastics pollution and the vast potential of waste plastics, Raman spectroscopy is not a readily available solution.

A reliable identification and sorting system that would rapidly identify waste plastics irrespective of the surface condition is highly desirable. Such system would be useful in developing nations were municipal solid wastes (MSW) are not separated at source, rather dumped to form an heterogenous mix. The system would enable an accurate separation of valuable waste products like polyolefin plastics (for pyrolysis), recyclable plastics, etc.

This paper aims to present a reliable waste plastics sorting method. First, a versatile NIR spectroscopy system that consists of inexpensive hardware and an adaptable calibration software is presented. The system can identify at least seven different polymers including multilayered waste plastics. Furthermore, a statistical analysis of the measurement result to determine the reliability of the system to separate polyolefins in different plastics conditions is also presented. The precision of the identification system was calculated using R-program's proportion testing[2] (prop test) [23]. This further establishes the influence of statistics on imaging science and its different application areas.

There are several systems that rely on near-infrared radiation sensors for waste plastics classification, most are available on the

[1] Polyolefins are a family of polyethylene and polypropylene plastics that are produced mainly from oil and natural gas. [34]

[2] A proportion test is used to test for the probability of success/ failure within a given proportion.

market. However, due to propriety knowledge protections, technical details are often unknown. The main contribution of this study is to investigate the potential of NIR spectroscopy in the identification of post-consumer plastics in different surface conditions. This is carried out while underlining the versatility of the proposed system.

This paper is structured as follows: Section 2 describes the types of materials and conditions investigated. Section 3 presents the classification calibration results showing the spectral information acquired from the image of the samples. Additionally, the statistical result is also presented in this section. The paper is concluded with a summary of the result, potential limitations that need further investigation and some remarks.

Materials and Methods

Post-consumer samples utilized

In this study, post-consumer plastics samples of HDPE, LLDPE, LDPE, PP, PET, PVC, and PS were collected from different sources. The plastics were identified by the recycling code at the bottom of the plastics. The plastics samples consisted of cut-out pieces of different sizes *(indicated in table 2 as acronym 'P')*, colors and composition *(see table 2)*. This was to investigate the influence of these attributes to the sorting efficiency and the versatility of the sorting system. Additionally, some end-of-life plastics in their manufacturing form were also utilized. A total of 210 plastics samples were selected and used for this study. Some of the samples were re-used in each condition to make up the number of required sample size for measurements in a condition. The samples were grouped and characterized based on their origin, color, and density *(see table 2)*. The variations in density values for each polymer is shown in table 2. Each value represents the arithmetic average of 2 independent measurements. The narrow values between the densities of some polymers like PS from HDPE, demonstrates the viability of the multispectral optical sorting system over systems that separates based on density.

Table 2: List of samples investigated in this study (source: compiled by author).

Name	Description	Sample origin	Color	Density (g/cm3)	No. of pieces
PET	Cooking-oil bottle	Waste plastics	Clear	1.39	6
PET-P	Coca-Cola bottle pieces	Waste plastics pieces	Clear	1.38	19
PVC	End-of-life plastics infusion bottle	Used plastics waste	White	1.35	3
PVC-P	Cut-outs from waste PVC plastics	Pieces from used plastics	White	1.40	17
PP	End-of-life yoghurt cups	Waste plastics	Off-white	0.92	7
PP-P	Pieces from waste PP plastics	Waste plastics pieces	Off-white	0.92	18
PS	Used take-away food packaging	Waste in plastics	White	1.05	4
PS-P	Cut-outs from waste plastics	Waste plastics pieces	White	1.05	16
HDPE	Bottle packaging	Waste plastics	Mixed	0.95	3
HDPE-P	Cut-outs from waste HDPE plastics	Waste plastics pieces	Mixed	0.96	22
LDPE	End-of-life detergent packaging	Waste plastics	Mixed	0.91	8
LDPE-P	Pieces from waste plastics	Waste plastics pieces	Mixed	0.92	17
LLDPE	Plastics waste shopping bags	Waste plastics	Mixed	0.87	8
LLDPE-P	Pieces from waste plastics	Waste plastics pieces	Mixed	0.88	22
Unknown	Not classified	Waste plastics pieces	Mixed	Varying	40

The surface conditions of the plastic were simulated to represent waste collection or landfills condition in urban-cities in West-Africa (specifically Kumasi, Ghana). 6 conditions were simulated namely: DRY – The samples were washed and dried and utilized in their cleanest form (*see figure 1 (a)*); WET – The samples were sprinkled -with or dipped-in water (*see figure 1 (b)*); LABELS – The samples were covered or partially covered with their manufacturing labels (*see figure 1 (c)*); Three levels of contamination were analyzed namely: contamination with a mixture of ketchup[3] (70%) and soil[4] (30%) – The contaminant was rubbed on the surface of samples (*see figure 1 (e)*); contamination with a mixture of mayonnaise[5] (70%) and soil (30 %) – The contaminant was rubbed on the surface of the plastics samples (*see figure 1 (d)*); contamination with a mixture of mayonnaise (40 %), ketchup (40 %) and soil (20 %) – The plastics samples were either partially or fully-immersed in the contaminant solution (*see figure 1 (f)*).

[3] **Ketchup** is a 'soft solid' made from a suspension of pulverized tomato solids in liquid [35].

[4] **Soil** is a solid mixture composed of minerals, organic matter, living organisms, gases and water [36].

[5] **Mayonnaise** is a semi-solid oil in water emulsion made of vegetable oil, vinegar, egg yolk (emulsifier), salt, and sugar [37]

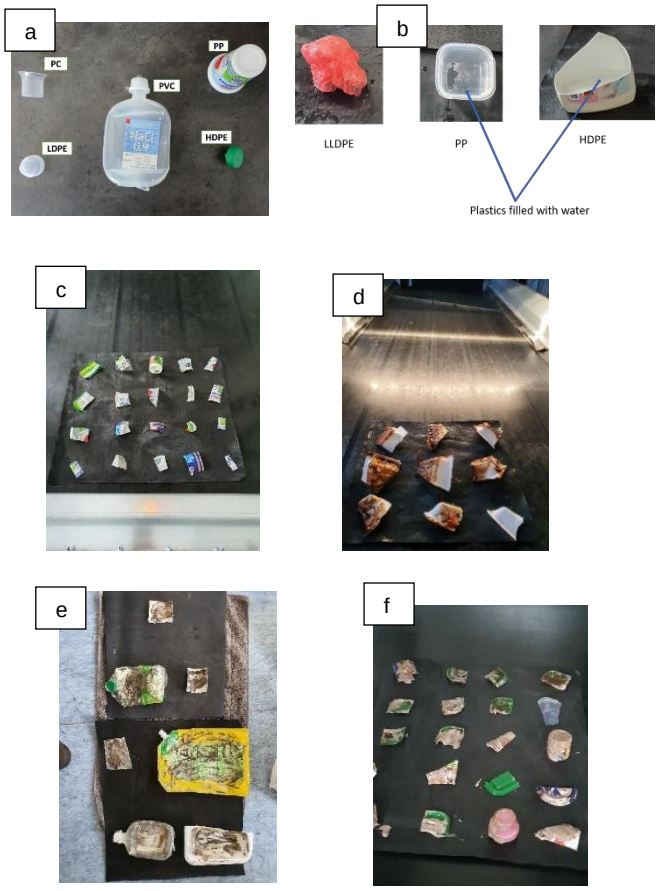

Figure 1: (a) dry samples; (b) wet samples; (c) samples with labels; (d)samples contaminated with a solution of mayonnaise and soil; (e) samples contaminated with a solution of ketchup and soil; (f) samples contaminated with a solution of ketchup, mayonnaise, and soil.

The sorting system

The multiplexed NIR spectrometer system used in this study was developed and manufactured by LLA Instruments. It is based on a system that first acquires a multispectral image of the material on the belt, and further evaluates the image to real-time classification data visualized in the software. The system allowed sampling within the spectral range of 1360nm - 1940nm. The system was employed to detect the behavior of chemical bonds in a polymer to photons from a lighting source. Each behavior is useful to identify the functional group of chemical bonds present in polymers. Also, each polymer type has unique functional groups that are used to identify the polymer [24].

The complete system was made up of both hardware and software. The hardware consisted of the transport unit, illumination unit, detection and spectral acquisition unit, and ejection unit as described below, while the software processed the image, and its operation is described in *the calibration results* section of this paper.

The transport unit incorporated a black-colored conveyor belt with a width and length of 1.45m x 3.0m, respectively *(see figure 2 (a))*. It is fitted with a single phase 1HP AC induction motor to deliver a speed of 3m/s. However, the measuring width in this study was 0.725m.

The illumination unit consisted of double-sided reflectors equipped with 120W/230V halogen lamps with a 50cm vertical clearance from the conveyor-belt *(see figure 2 (d))*.

The detection unit utilized several fibre-optic probes. The probes were arranged in a line at a pitch of 20mm *(see figure 2 (c))* The probes were connected via optical fibre cables to a 64 track optical multiplexer imaging the fibre channels at a scan rate of 50Hz onto the entrance slit of the NIR Spectrometer (KUSTA 1.9MPL-24V) *(see figure 4)*. The spectrometer consisted of a spectrograph with high spectral resolution of 4nm/pixel, and a linear sensor InGaAs camera. The camera had an integrated 16bit RGB sensor which was used for color detection and object positioning which was relevant for sample identification and ejection. The images presented in this study were acquired with a scan rate of 50Hz, spectral resolution of just below 8nm and a dispersion per pixel of 4nm. Additionally, 32 probe scanners were used to detect images in this study, hence, the conveyor-belt measuring width utilized was 725mm *(see figure 2 (a))*.

The ejection unit consisted of a pneumatic device that was attached to the end of the conveyor belt *(see figure 2 (b))*. It was positioned to blow identified samples (ejected samples) upwards into an ejected box, while the rejected samples naturally rolled into the rejected box.

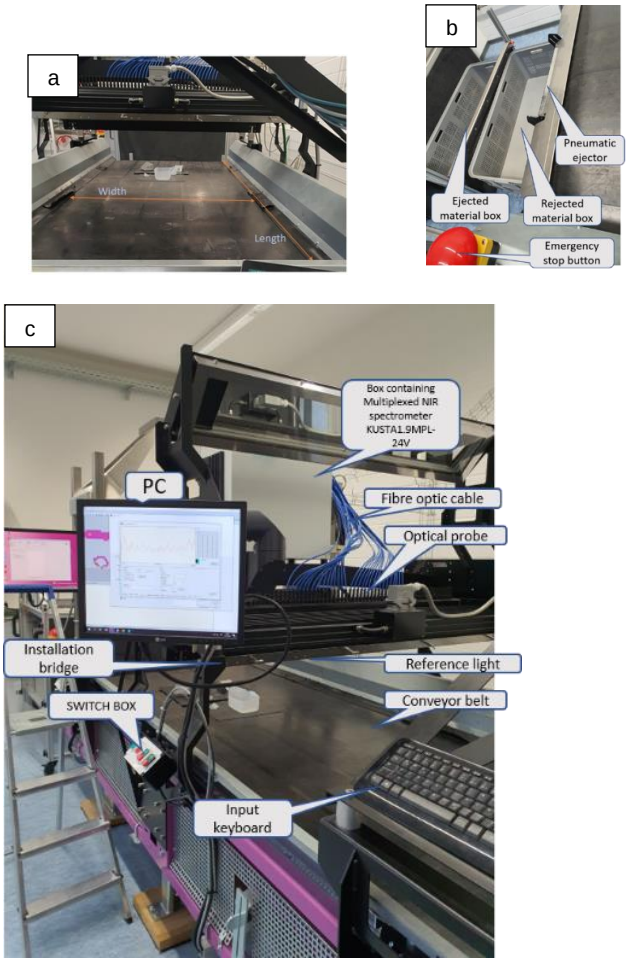

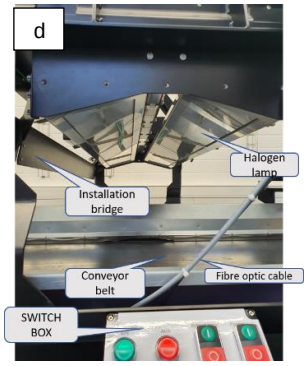

Figure 2: (a) transport unit; (b) ejection unit; (c) Complete diagram of the sorting system (front elevation); (d) cropped diagram showing the illumination unit and probe scanners.

The schematic of the information flow for the sorting system is illustrated in figure 3 (a) while the information flow for the spectrometer is represented in figure 3 (b) [25].

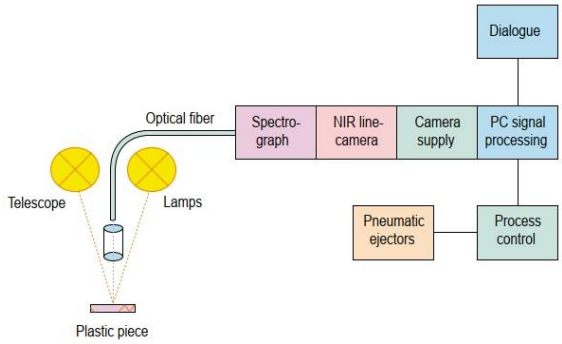

Figure 3: Schematic diagram of the NIR spectrometer used for identification (source: [26]*).*

Methodology

Near-infrared imaging is based on the principle that a material has a unique spectral signature, also known as a spectral fingerprint. The differences in the reflection, scatter, and absorption of the electromagnetic waves can be classified in characteristic patterns at distinct wavelengths due to the measured object's chemical composition and physical structure [27]. An image can be analyzed using an individual or a combination of different wavelengths. Since a single spectrum does not contain sufficient information to represent the material and perform its classification thoroughly, the system combines multiple bands in one data set. The process of the imagery acquisition, system calibration, and image classification are explained in this section.

Imagery acquisition

The multiplexed NIR system combines two types of sensors, InGaAs and CMOS, to detect visible and near-infrared light. This configuration enables the detection unit to provide the target's physical, geometrical characteristics (i.e., shape, size, position, and color), and the chemical composition through spectral analysis [27]. The schematic of the signal flow for the spectrometer is represented in figure 4.

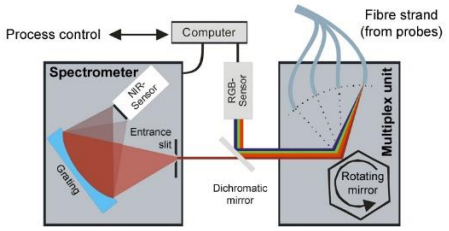

Figure 4: Schematic layout of KUSTAMPL system with integrated RGB sensor (source: [25]*)*

The detection unit with 32 probe-scanners is placed above the conveyor belt covering its entire width. A double-sided halogen lamp is a primary source providing light on the plastic sample. This concept minimizes shadowing and increases detection accuracy [28]. The intensity of the radiation reflected by the surface of the measured object depends on the type of plastic. The reflected light is transmitted to the spectrometer using NIR fibre optics that can be included in a probe line or installed separately, many meters apart [28]. The spectrometer possesses only a single input slit and can handle only one measurement point at same time. Since the processing for material detection needs more information, an optical multiplex unit is required. A multiplexer is a hardware component on the transmitter side for switching the measured probes to the spectrometer's entrance slit [28]. The task of the dichromatic mirror is to separate near-infrared light from the visible one. The spectrometer itself is integrated with a specially designed holographic concave grating and the infrared linear detector array [26]. The grating effect is to narrow down the spectrum, thus allowing a more precise determination of peak positions [29].

In this design, a one-dimensional linear NIR sensor is used to detect the reflected light spectrum. The row of pixels of the sensor represents the spectrum of one spatial point (optical track). Since the tracks are scanned at a rate of 50Hz (each) by the optical multiplexer, and the fibre optics probes are oriented in a line perpendicular to the conveyor belt's moving direction, the material is scanned by the line [25]. This process is comparable to the push-broom method, also known as line scanning imaging, this is also used in hyperspectral systems, where the camera records a whole row at once. Multiple lines are combined to reconstruct a three-dimensional scene, called a hyperspectral cube. Two dimensions (X and Y) represent the spatial information, and the third dimension the spectral data. The multiplexed system instead scans the conveyor belt channel by channel using fibre-optics as transmitters. A minimal time delay between the measured points, especially the first and last one, is present due to the spectrometer's input signal limitation, making the combining process of the scanned data even more challenging. However, this time delays are rarely apparent in use for the identification of plastics from household waste.

For the analyzing part, the analog-digital-unit (ADU) frame grabber converts the analog into a 16bit digital signal. Herewith, the physical information about the reflection's intensity is represented by an integer number with a maximal possible value of 16^2 transferred to the computer for further analyzing processes. The higher the ADU resolution, the more precise the measurement and, consequently, the detection is. Similar spectral signatures are associated with the same class. This allows defining a spectral library or set of reference spectra. Through the analysis of the

spectra, it is possible to recognize, and then classify, the different materials. Finally, due to characteristics in NIR-absorption bands the plastic type is recognized and given as an electronic code (EC). The EC, containing information of the sample's position on the belt, is fed into the process control, which is linked to pneumatic ejectors [30].

This system, in contrast to many hyperspectral imaging systems on the market, offers a very short measuring time, a high sensitivity, and a high spectral resolution. Thus, the configuration is very well suited to conveyor belt systems, where the object is moving in respect to the imaging unit [30][26].

Calibration

The acquisition system does not register the material reflectance but rather the intensity of the reflected radiation that reaches the camera sensor with an energy amount sufficient to be detected [27]. Furthermore, these measured values are affected by many factors that can produce significant errors in the interpretation of the extracted information [31]. Therefore, accurate calibration is a fundamental part of the analyzing process to guarantee the correctness of the image classification.

In practice, there are two standard methods of calibration [31]. In the first case, the calibration is based on the comparison of two additional images: a very bright image and a dark image representing the upper and lower limit of the intensity. The second method, which was implemented in this study, is related to the reference object visible in the analyzed sample. According to the spectra of high reflectance standard materials (~100% reflectance), the raw data will be transformed into the reflectance units. It is essential to isolate external conditions like ambiance dust, ambiance lighting, the conveyor belt color, and other factors [29]. This operation establishes the portion of the sensor that is useful in building the required spectral graph. The system was calibrated using a high-density fluoropolymer panel (Spectralon), assumed as Lambertian surface [11]. It is used as a white reference to retrieve spectral signatures on reflectance values. The Spectralon was placed on the conveyor belt at the measuring line and illuminated using the halogen lamps. The reference limits were then set [29].

According to the manufacturer LLA Instruments GmbH [28], automatic calibration is possible. The additional calibration unit comprises support arms, the calibration line, a motor, and the electronic control unit. The motor controls the position of the support arm and moves the calibration line into the calibration plane. After the process is finished, the arm is moved back into the initial position out of the image. The whole procedure takes only a few seconds.

Dependent on the brightness of the sample material, three different calibration materials are available [30]:

- bright - suitable for standard applications in paper and plastic recycling and bright (white) materials in general
- medium – suitable for darker materials such as gray rock
- dark – suitable for dark to black materials

Classification calibration results

In the overall classification results presented here, only coherent information points are explained while redundant information are set-aside. All the spectral diagrams are mean-centered and normalized mathematically, therefore the intensity scale are interpreted as arbitrary. As a first step, a single point classification algorithm has been applied, which utilized a partial least squares discriminant analysis routine (PLS-DA) [32]. Two filters were involved in improving the classification points, namely:

Object evaluation (image filter) which is a statistical deep-learning algorithm that utilizes K-Nearest Neighbor to predict the attribute (pixel-points represented by colored square boxes) of a point based on the attribute of the neighboring points. Further details of the concept is explained by [33].

Object-flip uses statistical methods to detect the attribute that possesses statistical majority point within an object. It then flips other points within the object to that attribute.

Results and Discussions

In this section, the calibration results and the measurements results are both presented. Additionally, statistical analysis of the measurement results is carried out and presented. A sample size of 60 measurements per condition were carried out for the DRY, WET and LABELS conditions, whilst 30 measurements per condition were performed for the 3 levels of plastics surface contamination. (described in the *Materials and Methods* section above). All subgroups of PE (HDPE, LDPE and LLDPE) are classified as PE.

The unique absorption peaks for each polymer type were found to be:

PET spectral indices (nm) – 1420, 1660, 1910.
PVC spectral indices (nm) – 1418, 1715, 1740.
PE spectral indices (nm) – 1415, 1720, 1760.
PP spectral indices (nm) – 1630, 1710, 1725.
PS spectral indices (nm) – 1640, 1680, 1760.

The results from this investigation are presented in two parts. The first part shows some classification calibration results for the different conditions simulated. Here, the representative spectral characteristics of selected polymers showing the effects of the contaminants are illustrated. Furthermore, the second part shows the statistical analysis of the classification results. Here, the accuracy and precision of the technique is computed based on the measurement results.

Results for Dry samples

Figure 5 (a) shows the visualization result of dry (clean) HDPE polymers. It illustrates the pixel-points formed from the unique absorption features of PE. The pixel-points (attribute) for all the objects were correctly classified as PE. This is demonstrated by the spectral graph of figure 5 (b). It compares the spectral features extracted from the points within the area of the black ellipse in figure 5 (a) with a reference spectrum of clean PE.

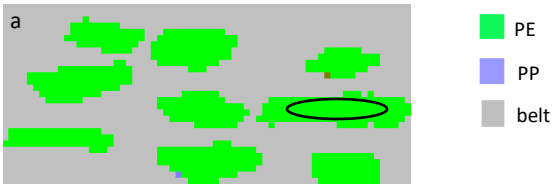

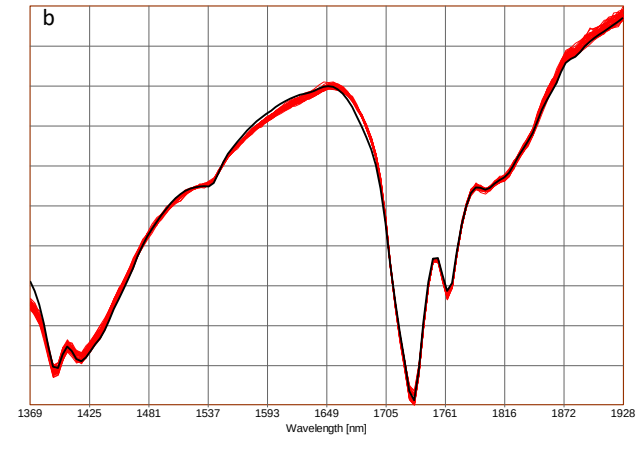

Figure 5: (a) Visualization result for HDPE samples; (b) Spectral graph showing points within the ellipse in figure 5 (a).

It is already evident here that all the absorption features of the HDPE samples match with the reference spectrum from the training set. Hence, there was no need to apply a filter to improve identification. Most of the samples in the DRY condition showed similar matching features when compared with their training sets. However, multi-layered, and composite materials in this condition required filter to improve their classification, this is illustrated in figures 6 (a – c).

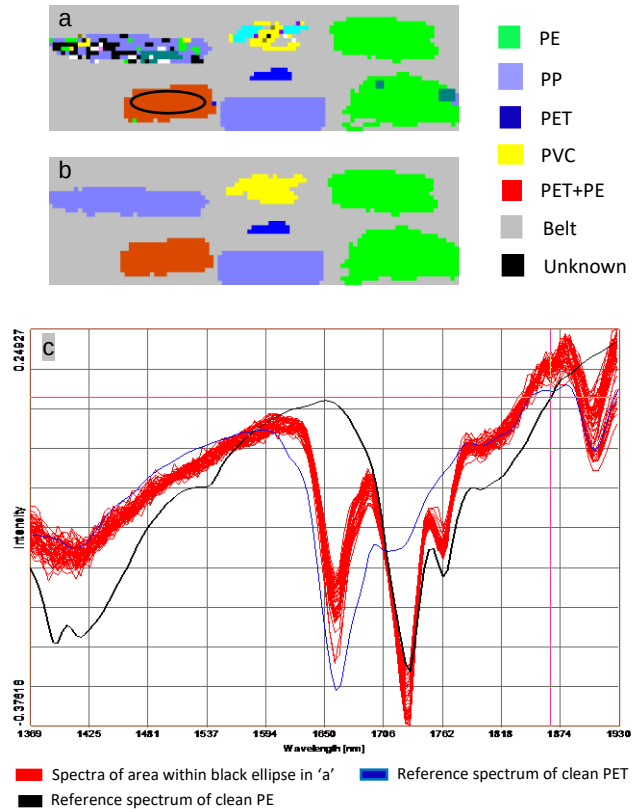

Figure 6: (a) Single point classification results of mixed dry samples; (b) classification results after applying object evaluation filter; (c) comparison spectra of points within ellipse in figure 6 (a) with reference spectra of dry PE and PET samples.

The red curves in figure (6 (c)) showing points within the area in the ellipse of figure (6 (a)), completely matches neither of the reference spectrum of PET nor PE. However, it shares features of PET at 1420 nm and 1660 nm, it also has corresponding features of PE at 1660 nm, 1720 nm, and 1760 nm. Consequently, the object is classified as a composite material made of PET and PE. The multilayered samples showed strong interference effects which disturbed the classification. It was therefore represented by multi-attributes shown by the differently colored pixel points in figure (6 (a)). An object evaluation filter was utilized to improve the pixel points for the objects and the results are displayed in figure (6 (b)).

Results for wet samples

Figure (7 (a)) shows some HDPE samples that wetted with water, some of the samples was partially filled with water. The classification results are shown in figure (7 (b)). It indicates that the although the influence of water molecules is strong, (evident in the missing pixel-points in some of the objects as shown by the arrow labeled 'Y' in figure 7 (b)), it does not affect the classification of the polymers. This is demonstrated by the spectral graph in figure 7 (d). The spectra of some points in the one of the WET HDPE sample are also illustrated. The points represented, are highlighted by the red ellipse in figure (7 (a)).

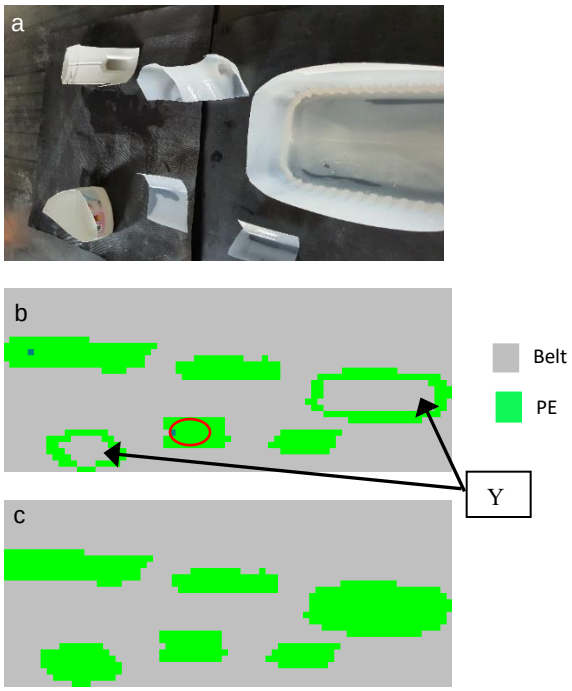

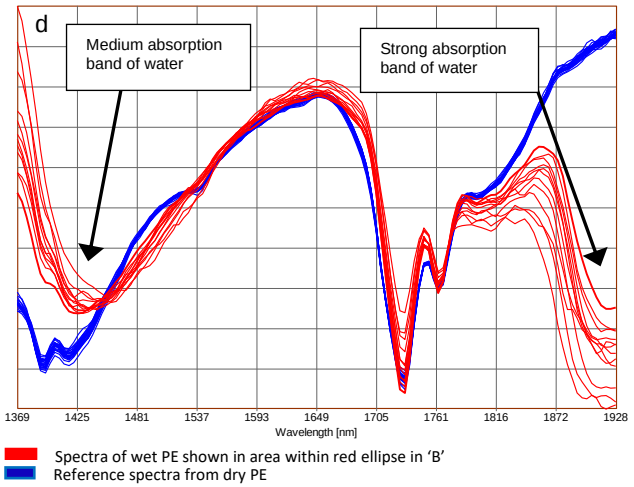

Figure 7: (a) Picture of wet HDPE samples on conveyor belt; (b) single point classification results of samples in figure 7 (a); (c) classification results after applying object evaluation; (d) comparison of reference PE spectra with spectra of points within red ellipse in figure 7 (b).

The red curves show the absorption bands of water, 1430 nm is the medium absorption band while 1920 nm is the strong absorption band. This influence of water does not affect the identification of the polymer as the water mostly absorbs the radiation in the 1st overtone. The fundamental mode ROIs of PE clearly matches with the reference spectra as indicated at 1720 nm, and 1760 nm. After applying an object classification filter, the missing pixel-points were all filled as shown in fig. 7 (c) and the objects were all correctly classified.

Results for samples with labels

Figure 8 (a) displays some of the samples with labels. Most samples with labels are multilayered (the labels are made from different polymer types). The effect of this is evident in the classification result shown in fig. 8 (b), which illustrates mixed pixel-point attributes (colors). This indicates the heterogeneity in the spectral features. However, the filters perform a major role in the identification of polymers in this condition. Figure 8 (c) shows improvements in the pixel-points after applying object-flip filter. All other objects were correctly classified after using the filter except one object which was wrongly classified as paper. However, this could be corrected if the 'PAPER' classification type is removed from the types of polymers to be analyzed in the classification tree.

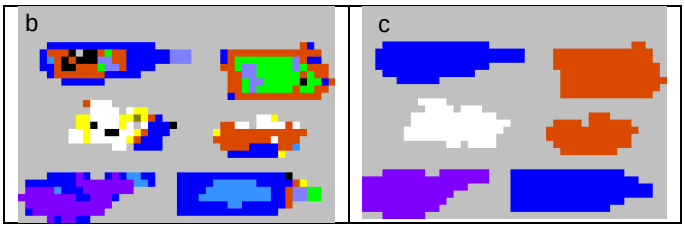

Figure 8: (a) Pictures of PP samples with production-labels on conveyor belt; (b) single point classification results of samples in figure 8 (a); (c) classification results after applying object-flip filter.

Figures 9 (a - d) shows the results of analyzing PP in this condition. Here there was no misclassification as the labels on the polymer had no influence on the identification. This is illustrated in the comparison spectral graph of fig. 9 (d). Which shows that all the absorption peaks from the objects matched those from the reference PP spectrum.

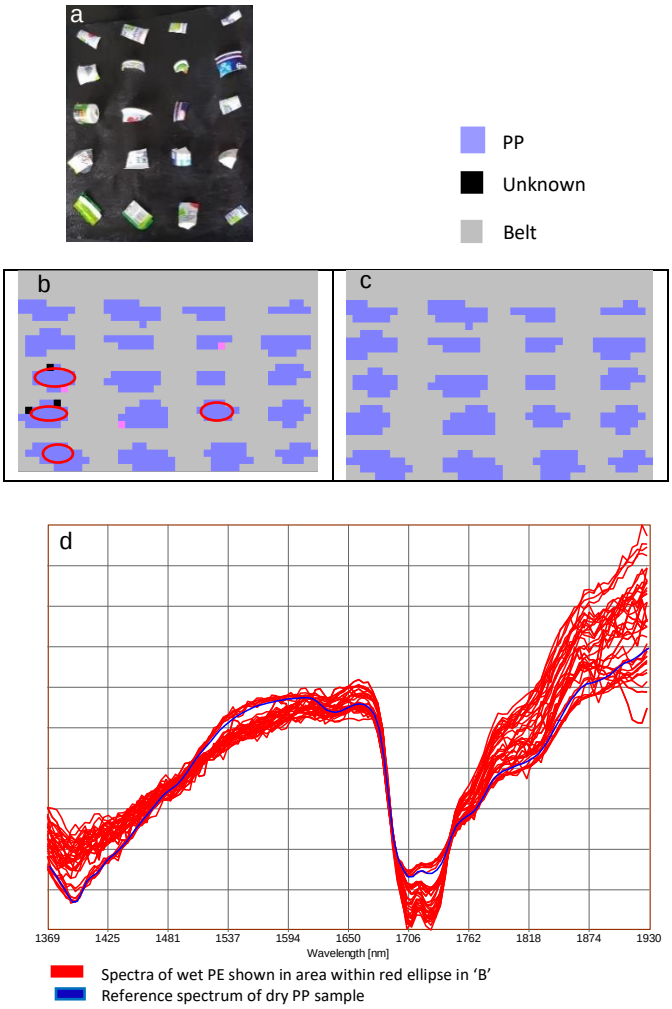

Figure 9: (a)Picture of PP samples with labels; (b) single point classification results of samples in figure 9 (a); (c) classification results after applying image filter; (d) comparison spectra of points within red ellipses in figure 9 (b) with reference PP spectrum.

Results for contaminated samples

Samples contaminated with a mixture of mayonnaise and soil: The results as presented, are some LLDPE samples that were contaminated with a mixture of mayonnaise and soil as illustrated in figures 10 (a -c). The initial classification results of LLDPE samples in this condition (as shown in fig. 10 (b)), signifies that most of the pixel-points were displayed as TETRA (green-colored pixel points). TETRA is a classification type, and it is a composite material made of PET and PE. Due to insufficient training sets of LLDPE in the chemometric library. Most of the features of the contaminated samples did not completely match with the spectra of PE (lemon-colored pixel points). Some points in the sample spectra were blurred out by the effect of the contaminant. However, it shared some unique features with TETRA. Consequently, some pixel-points were represented as TETRA as shown in fig. 10 (b).

After applying the two filters, some objects classification results were flipped to TETRA as shown in fig. 10 (c). Subsequent classification results of LLDPE improved significantly after adding more training sets to the library. This is evident in the total classification result in fig. 12(f).

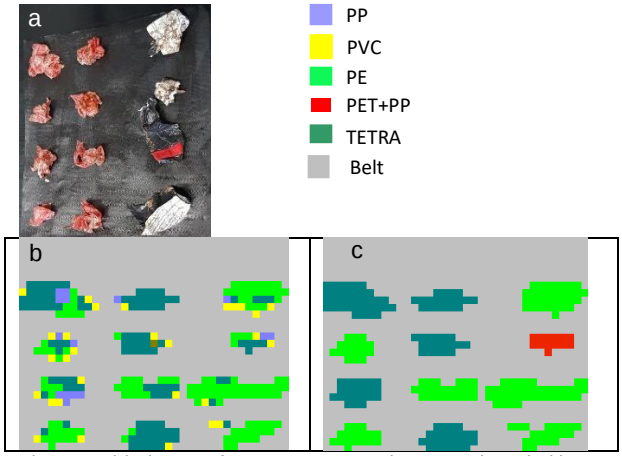

Figure 10: (a) pictures of some LLDPE samples contaminated with mayonnaise and soil; (b) single point classification results of samples in figure 10 (a); classification results after applying object filter.

Results for samples contaminated with a mixture of mayonnaise, ketchup, and soil:

Analysis of samples in this condition is illustrated in figures 11 (a – d). Few of the polymers had thick layers of contaminant on them as illustrated by the arrows labeled 'Z' in fig. 11 (a). This was to make more visible the effect of the contaminant on the classification (as this would be a prevalent condition if plastics wastes are mixed with organic wastes). The influence of the contaminant is obvious in the classification result shown in fig. 11 (b). It shows that some of the pixel points were represented as PVC (yellow-colored). The comparison spectral graph showing these effects is presented in fig. 11 (d). The points presented are highlighted by the blue ellipses in fig. 11 (b) and compared with the red ellipse in the same figure. It shows that the unique feature of PP at 1710 nm and 1725 nm (which is the 1st overtone of the C-H bond) has been completely blurred-out by the fat absorption in the mayonnaise. Thus, the feature now shares similarities with that of PVC (represented by the green curves). Hence, some pixel points of objects in the classification result are the attributes of PVC (yellow-colored pixel points) *(shown in figure 11 b)).*

Classification results for most of the PP samples were improved after applying object-flip filter as shown in figure 11 (c). However, there were few misclassifications of some objects. Overall, the results were promising.

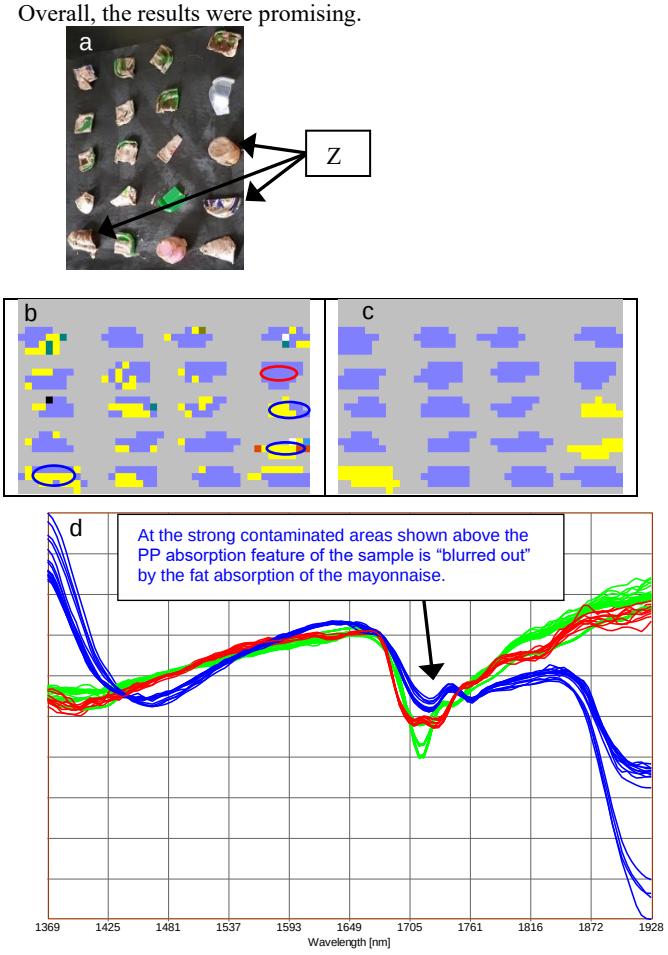

Figure 11: (a)Picture of contaminated PP samples; (b) single point classification results of samples in figure 11 (a); (c) classification results after applying object-flip filter; (d) comparison spectra of points within red and blue ellipses in figure 11 (b) with reference PVC spectra.

Statistics analysis of classification results.

The results for all the measurements carried out in the different conditions are presented in figures 12(a - f). The lowest misclassifications were obtained in the dry condition (*see fig. 12 (a)*) while the highest misclassifications were obtained when the samples were contaminated with a mixture of ketchup, mayonnaise, and soil (*see fig. 12 (f)*).

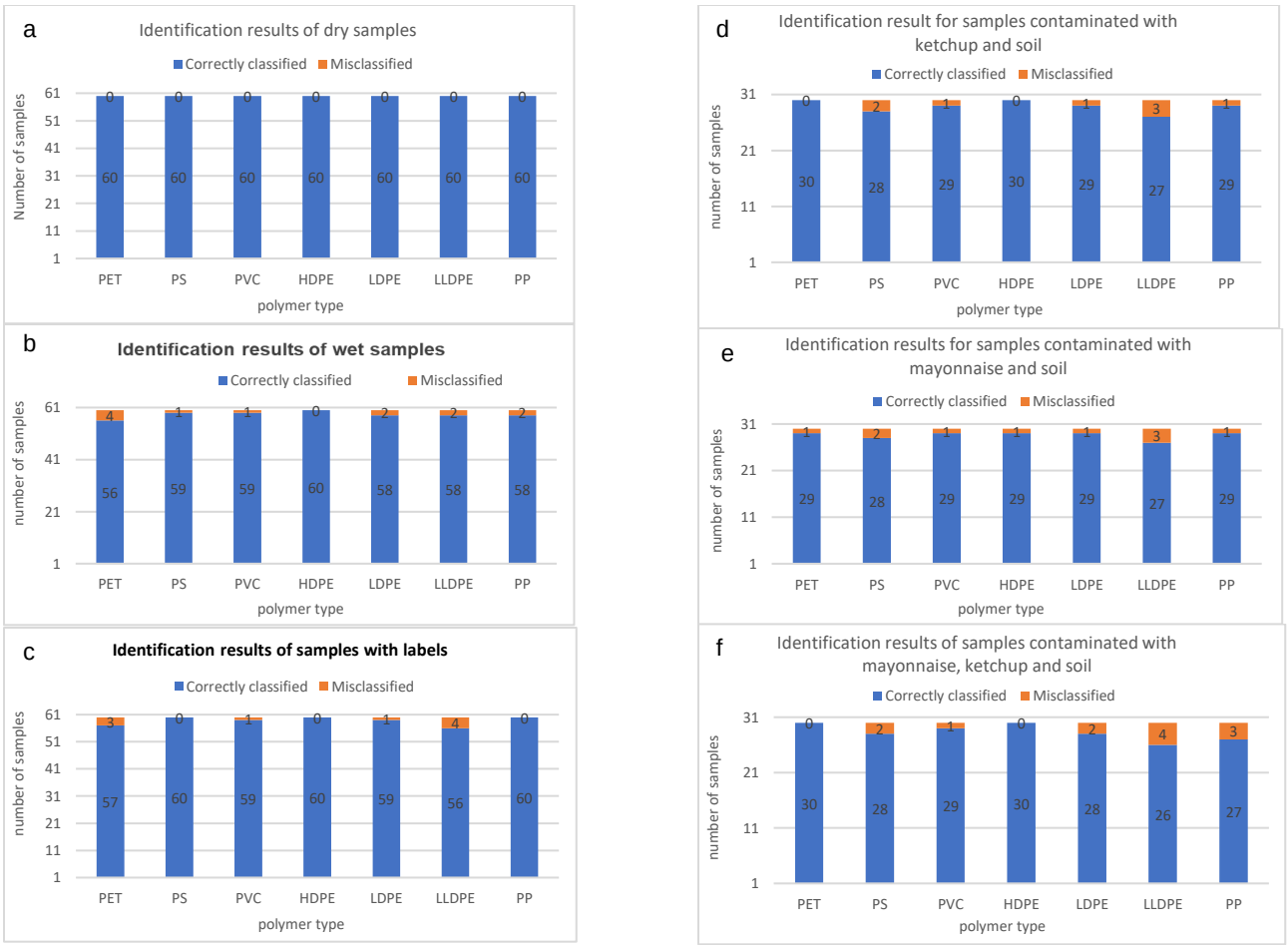

Figures 12 (a - f): Classification results of different polymers in six separate conditions.

Table 3: Precision boundary values (%) for polymers in different conditions with a 95% confidence level.

Condition	Polymer type						
	PET	***PS***	***PVC***	***HDPE***	***LDPE***	***LLDPE***	***PP***
Dry	0	0	0	0	0	0	0
Wet	83.0 - 97.8	89.9 - 99.9	89.9 - 99.9	0	87.5 - 99.4	87.5 - 99.4	87.5 - 99.4
Sleeve-label	85.2 - 98.7	0	89.9 - 99.9	0	89.9 - 99.9	83.0 - 97.8	0
Contaminated with ketchup + soil	0	76.5 - 98.8	80.9 - 99.8	0	80.9 - 99.8	72.3 - 97.4	80.9 - 99.8
Contaminated with mayonnaise + soil	80.9 - 99.8	76.5 - 98.8	80.9 - 99.8	80.9 - 99.8	80.9 - 99.8	72.3 - 97.4	80.9 - 99.8
Contaminated with ketchup + mayonnaise + soil	0	76.5 - 98.8	80.9 - 99.8	0	76.5 - 98.8	68.4 - 95.6	72.3 - 97.4

The statistical analysis of results computed using R-program.

The statistical analysis of the calibration results was computed using proportion testing (prop.test). It was carried out with the R-program. Prop.test is used to determine the error margin of the classification results. It has several potentials and can compute several arguments. Table 3 displays the precision boundaries (%) computed for the classification results with a 95% confidence interval.

The error margin was further calculated using *equation 1* below.

$$\text{Error margin} = \frac{\text{highest boundary of CI - lowest boundary of CI}}{2} \quad (1)$$

Where CI is the confidence interval, the higher value in each measurement in the table represents the highest boundary while the lower value represents the lowest boundary. Table 3 shows that the widest error margin was recorded by LLDPE in the condition (contaminated with a mixture of ketchup, mayonnaise, and soil). This is presumably due to the sample size and the number of misclassifications recorded by LLDPE in the stated condition.
Furthermore, the error margins were calculated, and the results were used to compute the precision of the technique in the classification of polymers in different conditions. The results are reported in table 4. Acronyms used in the table are: K-ketchup, M-mayonnaise, S-soil.

Table 4: Precision results (%) of NIR spectroscopy on polymer identification based on data analyzed in this study (with a 95% confidence level).

Condition	Polymer type						
	PET	**PS**	**PVC**	**HDPE**	**LDPE**	**LLDPE**	**PP**
Dry	100.0	100.0	100.0	100.0	100.0	100.0	100.0
Wet	90.4 ± 7.4	94.9 ± 5.0	94.9 ± 5.0	100.0	93.4 ± 6.0	93.4 ± 6.0	93.4 ± 6.0
Sleeve-label	91.9 ± 6.8	100.0	94.9 ± 5.0	100.0	94.9 ± 5.0	90.4 ± 7.4	100.0
Contaminated with K+S	100.0	87.7 ± 11.2	90.4 ± 9.4	100.0	90.4 ± 9.4	84.9 ± 12.5	90.4 ± 9.4
Contaminated with M+S	90.4 ± 9.4	87.7 ± 11.2	90.4 ± 9.4	90.4 ± 9.4	90.4 ± 9.4	84.9 ± 12.5	90.4 ± 9.4
Contaminated with K+M+S	100.0	87.7 ± 11.2	90.4 ± 9.4	100.0	87.7 ± 11.2	82% ± 13.6	84.9 ± 12.5

The accuracy values are the numbers preceding the ± sign while the error margins are the subsequent values (where the accuracy is the percentage of correct classification of polymers into their proper category). The highest precision as expected is recorded in the dry condition. Correspondingly, the lowest precision is recorded when the surfaces of the samples are contaminated in a mixture of ketchup, mayonnaise, and soil. Additionally, HDPE samples have the highest probability to be correctly identified in all conditions against other polymer types considered in this study. Conversely, the lowest average precision is recorded by LLDPE samples.

Accuracy assessment of NIR spectroscopy in the identification of polyolefins have also been computed. Polyolefins consists of all HDPE, LDPE, LLDPE and PP samples. The accuracy results are presented in figure 13 while the precision results showing the error margins (%) are illustrated in table 5. It shows that the highest accuracy was recorded when polyolefins are separated in the dry condition, while samples contaminated with a mixture of ketchup + mayonnaise + soil, conversely, have the lowest precision.

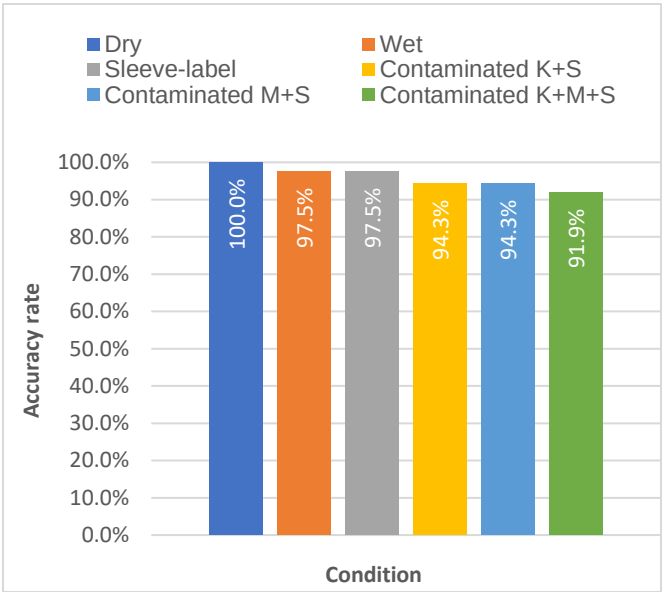

Figure 13: Accuracy of separation of polyolefins with a confidence level of 95%.

Table 5: Precision assessment of NIR spectroscopy in the separation of polyolefins (with a 95% confidence level).

Conditions	**Precision**
Dry	100.0%
Wet	97.5% ± 2.0%
Sleeve-labels	97.5% ± 2.0%
Contaminated with ketchup + soil	94.3% ± 4.2%
Contaminated with mayonnaise + soil	94.3% ± 4.2%
Contaminated with ketchup + mayonnaise + soil	91.9% ± 5.0%

Conclusion

The results in this study demonstrates that NIR spectroscopy is a suitable technique that could reliably identify, and subsequently, enable the separation of post-consumer PET, PS, PVC, HDPE, LDPE, LLDPE and PP polymers in different conditions. However, accurate classification depends on general factors such as the effectivity of classification filter, the spatial resolution of the spectrometer, lighting conditions, and even the competence of the operator. This study, additionally, shows that plastics can be separated with a high precision without sample preparation (such as washing and cleaning of waste plastics). The spectral range considered is 1369 nm - 1930 nm.

This investigation reveals that the highest precision is recorded when the samples are in the DRY condition, while

samples contaminated with a mixture of ketchup, mayonnaise and soil have the least precision. Unique absorption peaks for different polymers were found to be: *PET* – 1420 nm, 1660 nm, and 1910 nm; *PVC* – 1418 nm, 1715 nm, and 1740 nm; *PE* – 1415 nm, 1720 nm, and 1760nm; *PP* – 1630 nm, 1710 nm, and 1725 nm; *PS* – 1640 nm, 1680 nm, and 1760nm. Furthermore, it is observed that samples of the same polymer (irrespective of their sizes and colors (except black)), exhibits similar responses as disclosed by their spectral signatures.

Furthermore, this study shows that polyolefins can be separated with high precision. Polyolefins in the dry condition are identified with 100% precision while polyolefin samples in the wet and sleeve conditions are identified with high precision values of 97.5% ± 2.0%. Lastly, contaminated polyolefins are identified with precision values ranging from 94.3% ± 4.2% to 91.9% ± 5.0%. The results here indicate that NIR spectroscopy is effective in the identification of waste plastics polyolefins in different surface conditions. This investigation also seeks to stimulate the development of waste plastics separation systems in developing regions. Furthermore, it would facilitate each region to plan and develop a waste plastics management system based on their waste composition and energy requirement.

It is necessary to clarify that the sample size considered in this study may not be statistically sufficient. However, this is based on the scope and scale of implementation. Based on the calibration assessment conducted in this study, it indicates that the accuracy of identification would improve as more training sets from diverse sources (of post-consumer plastics) are introduced.

Acknowledgements

This research was supported by the German Ministry for Research and Education within the project "Waste to Energy: Hybrid Energy from Waste as Sustainable Solution for Ghana" (03SF0591E). The authors would also like to thank LLA Instruments GmbH & Co. KG (www.lla.de) for providing their NIR device which was used to carry out the tests. Finally, the authors appreciate SRH University of Applied Sciences, Berlin for providing a research stimulating environment that birthed this study.

References

[1] BIR, "BIR - Plastics," *BIR Annual Report*, 2019. https://www.bir.org/the-industry/plastics (accessed Oct. 06, 2020).

[2] Ellen MacArthur Foundation, "The New Plastics Economy: Rethinking the Future of Plastics & Catalysing Action," *Ellen MacArthur Found.*, no. January, p. 68, 2017, [Online]. Available: https://www.ellenmacarthurfoundation.org/publications/the-new-plastics-economy-rethinking-the-future-of-plastics-catalysing-action.

[3] J. O. Babayemi, I. C. Nnorom, O. Osibanjo, and R. Weber, "Ensuring sustainability in plastics use in Africa: consumption, waste generation, and projections," *Environ. Sci. Eur.*, vol. 31, no. 1, pp. 4–5, 2019.

[4] Hannah Ritchie and Max Roser, "Plastic Pollution - Our World in Data," 2018. https://ourworldindata.org/plastic-pollution (accessed Oct. 06, 2020).

[5] S. J. Thevenon, F., Carroll C., "Marine plastics | IUCN," 2020. https://www.iucn.org/resources/issues-briefs/marine-plastics (accessed Oct. 06, 2020).

[6] M. Cole and T. S. Galloway, "Ingestion of Nanoplastics and Microplastics by Pacific Oyster Larvae," *Environ. Sci. Technol.*, vol. 49, no. 24, pp. 14625–14632, 2015.

[7] L. Van Cauwenberghe, L. Devriese, F. Galgani, J. Robbens, and C. R. Janssen, "Microplastics in sediments: A review of techniques, occurrence and effects," *Mar. Environ. Res.*, vol. 111, pp. 5–17, 2015.

[8] Kirstin Linnenkoper, "Ready or not: plastics recycling 2.0 in Ghana • Recycling International," *Recycling International*, 2019. https://recyclinginternational.com/plastics/ready-or-not-plastics-recycling-2-0-in-ghana/27004/ (accessed Nov. 11, 2020).

[9] K. Miezah, K. Obiri-Danso, Z. Kádár, B. Fei-Baffoe, and M. Y. Mensah, "Municipal solid waste characterization and quantification as a measure towards effective waste management in Ghana," *Waste Manag.*, vol. 46, pp. 15–27, 2015.

[10] Global Recycling, "Plastic Recycling in Ghana – GLOBAL RECYCLING," *Mediaservice & Verlag GmbH*, 2019. https://global-recycling.info/archives/1984 (accessed Nov. 11, 2020).

[11] M. Moroni, A. Mei, A. Leonardi, E. Lupo, and F. La Marca, "PET and PVC separation with hyperspectral imagery," *Sensors (Switzerland)*, vol. 15, no. 1, pp. 2205–2227, 2015.

[12] J. Scheirs and W. Kaminsky, *Feedstock Recycling and Pyrolysis of Waste Plastics: Converting Waste Plastics into Diesel and Other Fuels*. John Wiley & Sons, Ltd, 2006.

[13] A. K. Panda, R. K. Singh, and D. K. Mishra, "Thermolysis of waste plastics to liquid fuel. A suitable method for plastic waste management and manufacture of value added products-A world prospective," *Renewable and Sustainable Energy Reviews 14*. pp. 233–248, 2010.

[14] D. D. Cornell, "Biopolymers in the existing postconsumer plastics recycling stream," *J. Polym. Environ.*, vol. 15, no. 4, pp. 295–299, 2007.

[15] E. A. Bruno, "Automated Sorting of Plastics for Recycling," 2000, [Online]. Available: http://www.p2pays.org/ref/09/08620.pdf.

[16] I. I. Inculet, G. S. P. Castle, and J. D. Brown, "Electrostatic separation of plastics for recycling," *Part. Sci. Technol.*, vol. 16, no. 1, pp. 91–100, 1998, [Online]. Available: https://doi.org/10.1080/02726359808906787.

[17] D. W. Sun, *Computer Vision Technology for Food Quality*

Evaluation: Second Edition. 2016.

[18] V. Allen, J. H. Kalivas, and R. G. Rodriguez, "Post-consumer plastic identification using Raman spectroscopy," *Appl. Spectrosc.*, vol. 53, no. 6, pp. 672–681, 1999, [Online]. Available: https://doi.org/10.1366/0003702991947324.

[19] M. Bukshtab, "Laser Spectroscopy," in *Springer Series in Optical Sciences, Vol. 163*, Springer, pp. 367–400, 2012.

[20] S. Brunner, P. Fomin, and C. Kargel, "Automated sorting of polymer flakes: Fluorescence labeling and development of a measurement system prototype," *Waste Management, Vol. 38*. pp. 49–60, 2015.

[21] D. Steele, "Infrared Spectroscopy: Theory," in *Handbook of Vibrational Spectroscopy, Vol. 1*, 1st ed., John Wiley & Sons, Ltd, 2006.

[22] N. Buzgar, A. I. Apopei, and A. Buzatu, "Advantages and disadvantages of Raman Spectroscopy," *Romanian Database of Raman Spectroscopy*, 2009. http://www.rdrs.ro/blog/articles/advantages-disadvantages-raman-spectroscopy/ (accessed Nov. 30, 2020).

[23] H. Barreto, F. Howland, H. Barreto, and F. Howland, "Confidence Intervals and Hypothesis Testing," in *Introductory Econometrics*, 2012.

[24] F. Vidal and F. Jäkle, "Functional Polymeric Materials Based on Main-Group Elements," *Angewandte Chemie - International Edition*. p. 131, 2019.

[25] A. Volland, "Multiplexed NIR spectroscopic Sensors and NIR spectro- scopic Imaging : Two Solutions for Sensor based Waste Sort- ing in Comparison Plastic identification with NIR NIR-sensors," no. 1, pp. 1–9, 2009.

[26] G. A. Gasparian and H. Lucht, "Indium gallium arsenide NIR photodiode array spectroscopy - Part II: Plastic waste sorting applications of a multiplexed NIR spectrometer," *Mol. Spectrosc. (Santa Monica)*, vol. 15, no. 4, pp. 14–17, 2000.

[27] G. ElMasry, M. Kamruzzaman, D. W. Sun, and P. Allen, "Principles and Applications of Hyperspectral Imaging in Quality Evaluation of Agro-Food Products: A Review," *Critical Reviews in Food Science and Nutrition*. pp. 999–1023, 2012.

[28] LLA Instruments, "Multiplexed NIR spectrometer - LLA Instruments GmbH & Co. KG," 2020. https://www.lla-instruments.com/spectrometer-cameras/multiplexed-nir-spectrometer.html (accessed Dec. 06, 2020).

[29] U. Bassey, "The potential of NIR Spectroscopy in the separation of plastics for pyrolysis," *Master Thesis*, 2020.

[30] and A. U. H. Lucht, L. Kreuchwig, "Plastic separation of automotive waste by superfast near-infrared sensors," p. LLA Instruments GmbH, 2000, [Online]. Available: https://www.lla-instruments.com/files/lla/pdf/Publikationen ENG/NIR_publications/Plastic_separation_automotive_waste_by_fast_NIR_sensors.pdf.

[31] R. Koprowski, "Processing of Hyperspectral Medical Images," 2017.

[32] H. Martens and T. Næs, "Multivariate calibration. I. Concepts and distinctions," *Trends in Analytical Chemistry*. 1984, doi: 10.1016/0165-9936(84)85008-6.

[33] G. Guo, H. Wang, D. Bell, Y. Bi, and K. Greer, "KNN model-based approach in classification," *Lect. Notes Comput. Sci. (including Subser. Lect. Notes Artif. Intell. Lect. Notes Bioinformatics)*, vol. 2888, pp. 986–996, 2003.

[34] PlasticsEurope Deutschland e.V, "Plastics – the Facts 2019," *PlasticsEurope*, 2019.

[35] N. Hannink, "Rheology," *Futurity*, 2016. https://www.futurity.org/ketchup-physics-rheology-1321922-2/ (accessed Nov. 12, 2020).

[36] B. A. Needelman, "What Are Soils?," *Nature Education Knowledge 4(3):2*, 2013. https://www.nature.com/scitable/knowledge/library/what-are-soils-67647639/ (accessed Nov. 12, 2020).

[37] J. A. Depree and G. P. Savage, "Physical and flavour stability of mayonnaise," *Trends Food Sci. Technol.*, vol. 12, no. 5–6, pp. 157–163, 2001.

Author Biography

Uduak Bassey (M.Sc.) is a Research Associate at Berlin School of Technology, SRH University of Applied Sciences in Berlin, Germany. He is also a Ph.D. candidate in University of Rostock, Germany and is on the research team of the project "Waste to Energy: Hybrid Energy from Waste as Sustainable Solution for Ghana."

Lukasz Rojek (M.Sc.) is a Ph.D. candidate at the University of Bamberg in the field of Geography. He is also a Research Associate at SRH Hochschule Berlin and guest lecturer at the Beuth University of Applied Science in the field of Surveying and Geoinformatics.

Prof. Dr. Michael Hartmann is the Academic Director of SRH Berlin School of Technology; Head of the Study Programs: Engineering and International Business; Engineering and Sustainable Technology Management.

Prof. Dr. Reiner Creutzburg is a retired Professor for applied computer science at the Technische Hochschule Brandenburg in Brandenburg, Germany. Since 2019 he is a Professor of IT Security at the SRH Berlin University of

Applied Sciences, Berlin School of Technology. He is a member of the IEEE and SPIE and chairman of the Multimedia on Mobile Devices (MOBMU) conference at the Electronic Imaging conferences since 2005. In 2019, he was elected a member of the Leibniz Society of Sciences to Berlin e.V. His research interest is focused on Cybersecurity, Digital Forensics, Open Source Intelligence (OSINT), Multimedia Signal Processing, eLearning, Parallel Memory Architectures, and Modern Digital Media and Imaging Applications.

Arne Volland is the product manager of LLA Instruments GmbH & Co. KG and a specialist in the development of sensor-based sorting solutions.

JOIN US AT THE NEXT EI!

IS&T International Symposium on

Electronic Imaging

SCIENCE AND TECHNOLOGY

Imaging across applications . . . Where industry and academia meet!

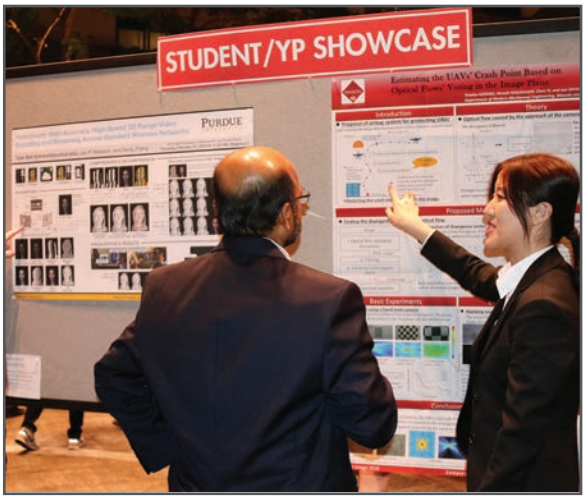

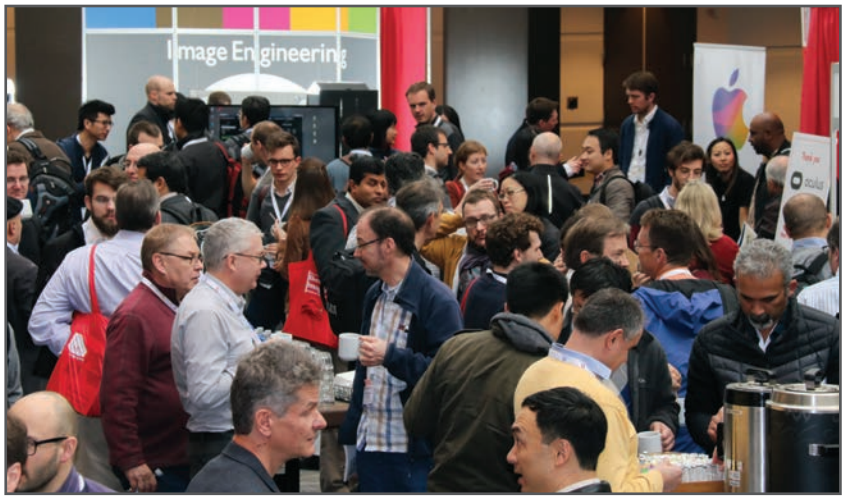

• SHORT COURSES • EXHIBITS • DEMONSTRATION SESSION • PLENARY TALKS •
• INTERACTIVE PAPER SESSION • SPECIAL EVENTS • TECHNICAL SESSIONS •

www.electronicimaging.org

IS&T
imaging.org